The 10th International Symposium on Flow Visualization
August 26-29, 2002, Kyoto, Japan
F0311

Winter Air Pollution Mechanism of Katmandu Valley by Water Tank Experiment

Shrestha, M. L.*[1], Kaga, A.*[2], Kondo, A.*[2], and Inoue, Y.*[2]

*1 Department of Environmental Engineering, Osaka University,
2-1, Yamada-Oka, Suita, Osaka 565-0871, Japan
Tel: +81-6-6879-7670 / FAX: +81-6-6879-7669
E-mail: manohar@moon.env.eng.osaka-u.ac.jp
*2 Department of Environmental Engineering, Osaka University, Osaka, Japan

Abstract: The air pollution concentration in winter season is found higher than summer season due to the formation of inversion layer in Kathmandu valley. This mechanism was simulated by water tank experiment and numerical calculation. Thermal stratification was made at the beginning of the experiment and the surface temperature of valley model was changed with the period of 12 minute matching the field temperature of Kathmandu valley. The updraft wind and Bernard convection occurred during the daytime and downdraft wind and inversion layer were realized during nighttime. The flow field and temperature obtained in water tank experiment and numerical calculation qualitatively agreed.

Keywords: Kathmandu Valley, Water Tank Experiment, Inversion Layer, Flow Field, PIV

1. Introduction

Kathmandu, the Capital of Nepal has the altitude of approximately 1400m and is surrounded by mountains higher than 1000m from ground level of the valley. The atmospheric pollution in Katmandu is getting worse and is found to be higher during winter season. The authors measured the concentration of NO_2,TSP and temperature in Katmandu for two weeks (February 2001). It was found that the concentration of NO_2 (Fig. 1) and TSP (Fig.2) became high in the morning and a strong stable layer was formed from midnight to early morning [1]. The formation of inversion layer was verified by the vertical height temperature measurement in Kathmandu valley as shown in fig.3. The reverse temperature at day and night can be seen in Fig.3. The high atmospheric pollution concentration in the morning is strongly influenced by the stable layer as well as the increase of traffic volume in the morning. In this paper, we performed the water tank experiment [2], [3] and the numerical experiment for the atmospheric pollution in Katmandu valley and analyzed the mechanism of high atmospheric pollution concentration in the morning.

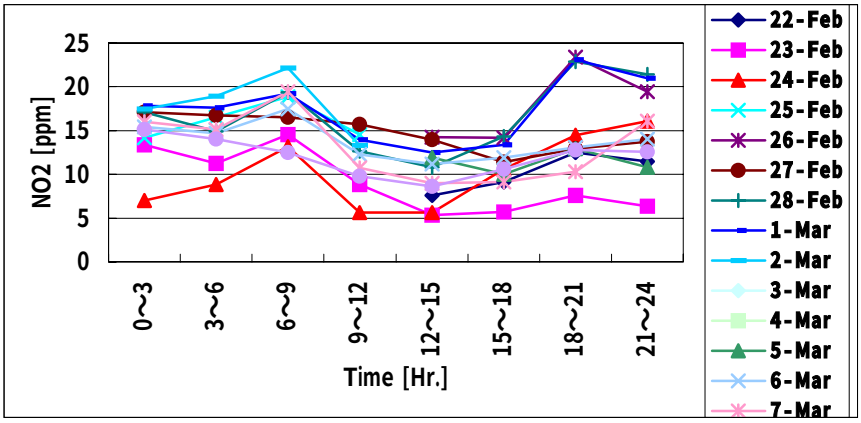

Fig.1. Diurnal variation of NO_2 at Kathmandu valley.

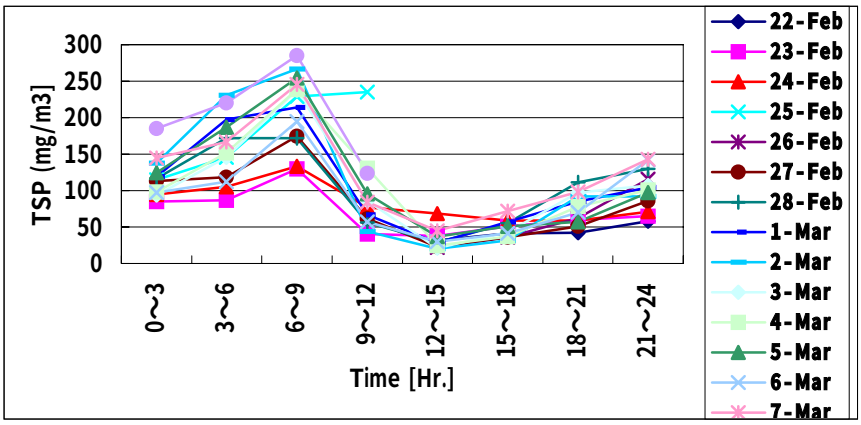

Fig.2. Diurnal variation of TSP at Kathmandu valley.

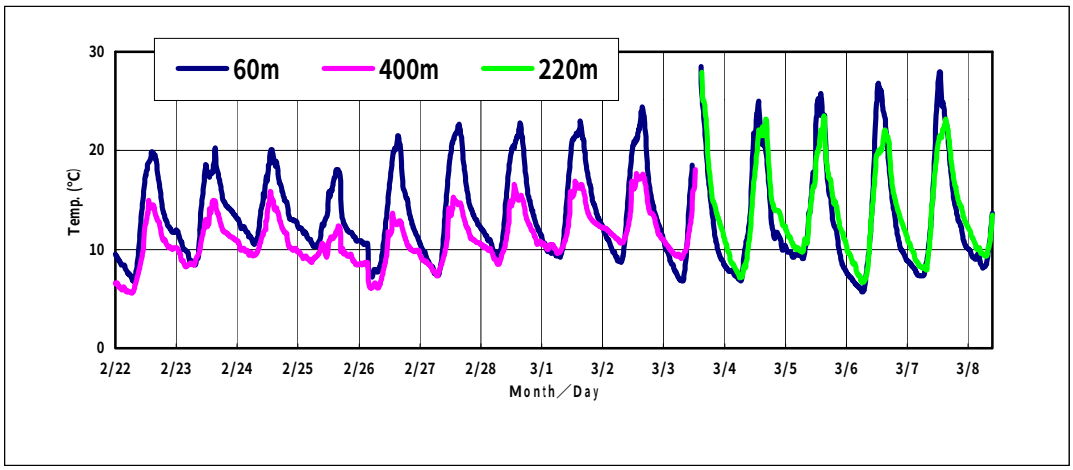

Fig. 3 Temperature measurement at 60m, 220m and 400m above Kathmandu valley

2. Water Tank Experiment

2.1 Experimental Equipment

The water tank experiment equipment is shown in Fig.4. This equipment consists of 3 water tanks. The middle water tank (500mm×400mm×70mm) was assumed as the atmosphere of Katmandu valley. The water temperature in the top tank was kept at a constant temperature but water temperature in the bottom tank changed with constant period and constant amplitude in order to change the lower surface temperature of the middle water tank which was assumed as the ground surface in Katmandu valley.

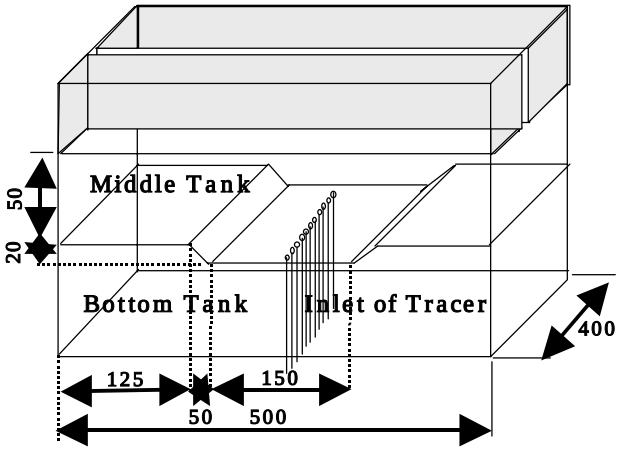

Fig. 4. Equipment for water tank experiment

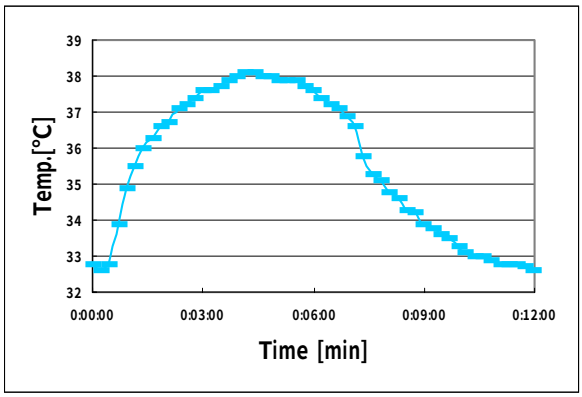

Fig 5. Variation of bottom temperature in the middle water tank

2.2 Experimental Method

Water temperature of the top tank was kept at 40 ℃. Simultaneously the water temperature of the bottom tank was kept at 35 ℃. After a few hours, the thermal stratification with constant temperature gradient was formed in the middle tank. Then, the lower surface temperature of the middle water tank was changed with the period of 12min as shown in Fig.5. This corresponded to the ground temperature variation of Kathmandu Valley for 24 hours during the month of February as shown in table 1. The measurements of temperature and flow field were carried out in that condition.

Table 1 Corresponding time of water tank experiment with field time (Kathmandu valley)

Expt. (min)	0	1	2	3	4	5	6	7	8	9	10	11	12
Field time	6 AM	8 AM	10 AM	12 AM	14 PM	16 PM	18 PM	20 PM	22 PM	24 PM	2 AM	4 AM	6 AM

2.2.1 Measurement of temperature

Thermo couples were used to measure the temperature in the middle tank at the height of 0, 5, 10, 15, 20, 40 and 60mm. The height of 20mm is approximately equal to the mountain height of Katmandu valley. The measured temperature and simulated results were also compared. The temperature distribution of whole valley region in water tank experiment was visualized by using thermo liquid crystal sheet.

2.2.2 Measurement of flow field by PIV

Styrofoam was made into fine particles by using electric mixer and suspended in water for 3 hours. The particles of Styrofoam having the same density as water were used as PIV tracer. These tracers were suspended homogeneously in the water of middle tank. After formation of temperature stratification, Ar laser beam was focused in the middle tank through the slit made in the top tank. Bottom temperature of the middle tank was changed as shown in Fig. 5 and middle tank was observed by using progressive camera. The 600 frames of images were taken up to 15 minute in interval of 1.5 second. The velocity vectors were calculated from the movement of tracer patterns between the visualized images [4].

Only half portion of the water tank experiment was photographed for better view. The flow field at the lower portion of the tank by PIV method is important in this experiment. But due to existence of slop and corner in the tank, the PIV analysis near the bottom becomes difficult. To solve this problem, regions used for the image analysis (Fig.6b) was converted into rectangular image (Fig. 6c) and extraction of vector was done in converted image and later, the vectors are brought to its original image. The coordinate of the image conversion was done by equation 1.

(a) Original Image (b) Analyzed Zone (c) Converted Image

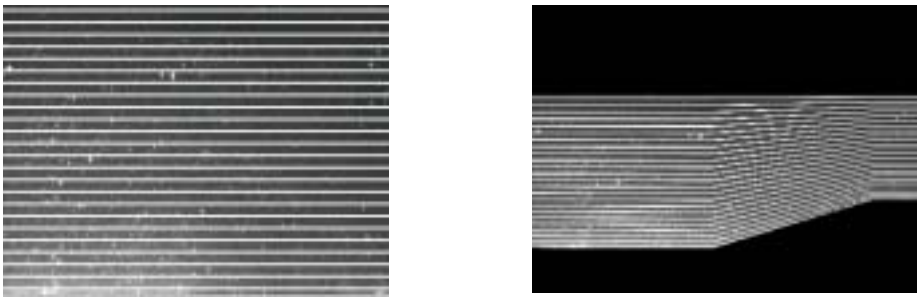

(d) Vertical Lines on Converted Image (e) Corresponding Lines on Original Image

Fig.6 Image Conversion for PIV at the Point Near Uneven

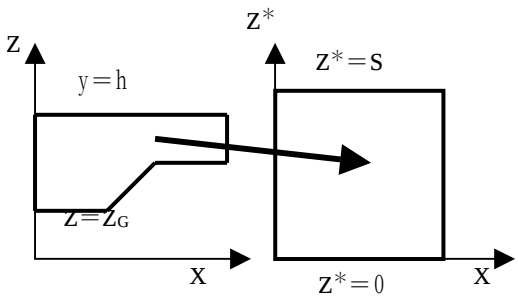

Fig 4 (b) Fig 4 (c)

Fig.7 The coordinate for Image Conversion

$$Z^* = S\left(\frac{Z - Z_G}{S - Z_g}\right)^m \quad (1)$$

Here, the value of m was taken as 0.9 and the lower analyzed region was enlarged comparatively than upper region [Fig.4 (d, e)].

2.3 Similarity rule

Ueda et al.,[5] proposed new dimensionless variables that may be the universal similarity variables for comparing with field-observation results.

$$U^+ = U^* G_r^{1/2} P_r^{2/3} \quad (2)$$

$$X^+ = X^* G_r^{-0.387} \quad (3)$$

$$Z^+ = Z^* P_r^{1/4} \quad (4)$$

Where U^* is the dimensionless wind speed, X^* and Z^* are the dimensionless length of the horizontal direction and the vertical direction respectively. G_r and P_r are Grashof and Prandtl number respectively. The representative wind speed and the representative length are defined by;

$$U = \frac{g\beta\Delta\Theta}{\omega} \quad (5)$$

$$L = \left(\frac{\gamma}{\omega}\right)^{\frac{1}{2}} \quad (6)$$

Where g is the gravitational acceleration, β is the volumetric expansion coefficient, $\Delta\Theta$ is the maximum temperature difference of the surface temperature variable, ω is the angular velocity of earth's rotation and γ is the eddy diffusivity of momentum.

Grashof number G_r and Prandtl number P_r are expressed by;

$$G_r = -\frac{g\beta.\Gamma L^4}{\gamma^4} \quad (7)$$

$$P_r = -\frac{\gamma}{\alpha} \quad (8)$$

Where Γ is the mean atmospheric temperature gradient and α is the eddy diffusivity of heat.

The typical values of α, β etc. in this experiment and in the field are shown in Table 2. The relation of horizontal length, vertical length and wind speed between this experiment and the field are calculated as shown in Table 3 by using the values of Table2. From the relation, the valley depth of 2 cm corresponds to 1112m depth of actual Kathmandu valley.

Table 2 Typical values of physical variables in the experiment and in the filed

	β [K^{-1}]	ν[m^2/s]	α [m^2/s]	ω[rad/s]	Γ [K/s]	$\Delta\Theta$ [K]
Experiment	0.000207	10^{-6}	1.43×10^{-7}	0.00873	100	5.6
Field	0.00341	10	10	$7.27\text{x}10^{-5}$	0.005	15

Table 3 Relation between experiment and field

	Experiment	Field
Horizontal length	1 [mm]	90 [m]
Vertical length	1 [mm]	56 [m]
Wind speed	1 [mm/s]	6.3 [m/s]

3. Numerical model for water tank experiment

3.1 Basic equations

The flow of water tank model is assumed to be 2 dimensional laminar flow. With the Boussinesq approximation, the following set of the basic equations for the water tank experiment were used.

$$\frac{du}{dt} = -\frac{1}{\rho}\left(\frac{\partial p'}{\partial x} + G_2\frac{\partial p'}{\partial z^*}\right) + \frac{\partial}{\partial x}\left(\nu\frac{\partial u}{\partial x}\right) + \frac{\partial}{\partial x}\left(\nu G_2\frac{\partial u}{\partial z^*}\right) + G_2\frac{\partial}{\partial z^*}\left(\nu\frac{\partial u}{\partial x}\right) + G_2\frac{\partial}{\partial z^*}\left(\nu G_2\frac{\partial u}{\partial z^*}\right) + G_1\frac{\partial}{\partial z^*}\left(\nu G_1\frac{\partial u}{\partial z^*}\right) \quad (9)$$

$< >$: operation of horizontal average

$$\frac{dw}{dt} = -\frac{1}{\rho}\frac{\partial p'}{\partial z^*} + \frac{< p > -\rho}{< p >} g + \frac{\partial}{\partial x}\left(\nu\frac{\partial w}{\partial x}\right) + \frac{\partial}{\partial x}\left(\nu G_2\frac{\partial w}{\partial z^*}\right) + G_2\frac{\partial}{\partial z^*}\left(\nu\frac{\partial w}{\partial x}\right) + G_2\frac{\partial}{\partial z^*}\left(\nu G_2\frac{\partial w}{\partial z^*}\right) + G_1\frac{\partial}{\partial z^*}\left(\nu G_1\frac{\partial w}{\partial z^*}\right) \quad (10)$$

$$\frac{du}{dx} + G_2\frac{\partial u}{\partial z^*} + G_1\frac{\partial w}{\partial z^*} = 0 \quad (11)$$

$$\frac{dT}{dt} = +\frac{\partial}{\partial x}\left(\alpha\frac{\partial T}{\partial x}\right) + \frac{\partial}{\partial x}\left(\alpha G_2\frac{\partial T}{\partial z^*}\right) + G_2\frac{\partial}{\partial z^*}\left(\alpha\frac{\partial T}{\partial x}\right) + G_2\frac{\partial}{\partial z^*}\left(\alpha G_2\frac{\partial T}{\partial z^*}\right) + G_1\frac{\partial}{\partial z^*}\left(\alpha G_1\frac{\partial T}{\partial z^*}\right) \quad (12)$$

$$Z^* = S\frac{Z - Z_G}{S - Z_G} \quad (13)$$

$$G_1 = \frac{\partial z^*}{\partial z} = \frac{S}{S - Z_G} \quad (14)$$

$$G_2 = \frac{\partial z^*}{\partial x} = \frac{Z^{*-s}}{S - Z_G}\frac{\partial z_G}{\partial x} \quad (15)$$

Where u, w, T and p are velocity at horizontal direction, velocity at vertical direction, temperature and pressure respectively. The prime is the deviation from the initial value.

S and z_G are the top height of region and the height of ground level.

ρ, γ and α. are density, kinetic viscosity and heat transfer coefficient of water.

ρ γ and α. are approximated by

$$\rho.[g/cm^2] = 0.05\times10^{-5}T_C^{\,2} + 1.02 \quad (16)$$

$$\gamma.[cm^2/s] = 0.046\times10^{-4}T_C^{\,2} - 0.438\times10^{-3}T_C + 1.0703\times10^{-2} \quad (17)$$

$$\alpha.[cm^2/s] = 0.003\times10^{-5}T_C^{\,2} - 0.062\times10^{-4}T_C + 1.31\times10^{-3} \quad (18)$$

Where,

$$T_C = T - 273$$

3.2 Calculation condition

The calculated region is the same as the x-z section of the experimental equipment (Fig.4). The calculation was done by dividing the region into 181 ×40 meshes. The boundary conditions are also the same as the experimental conditions.

4.Results

4.1 Temperature

The temperature distribution of the water tank experiment measured by thermocouples at the height of 5mm, 10mm, 15mm, 20mm, 40mm and 60mm, top tank and valley surface are shown in Fig. 8. The 0 minute corresponds to the time of sunrise of the field. The horizontal axis is from 0 to 12 minute which it is representing the field time scale for 24 hours. The change of the surface temperature pattern in experiment nearly resembled with the actual temperature pattern of the field. The amplitude of the valley surface is 5.5℃ in the experiment. The effect of the valley surface temperature change in the water tank experiment is up to 20mm vertical height which is equivalent to 1120m in the field. Again, it is known from Fig. 8 that the formation of inversion layer takes place from 7.5 minute to 1.5 minute of next day (21 pm to 9 am of next day).

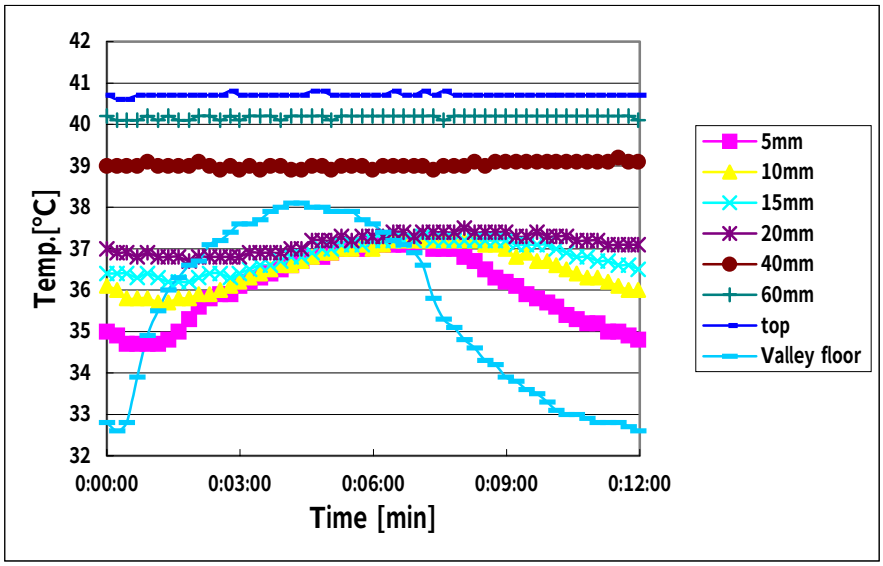

Fig. 8 Vertical temperature variation in Water tank

The temperature of the water tank experiment was visualized by using thermo crystal liquid sheet as shown in Fig. 9. The experiment was carried out making the surface temperature of valley as shown in Fig.5. The temperature distribution in water tank experiment can be seen in Fig.9 and horizontal level possesses the same temperature level.

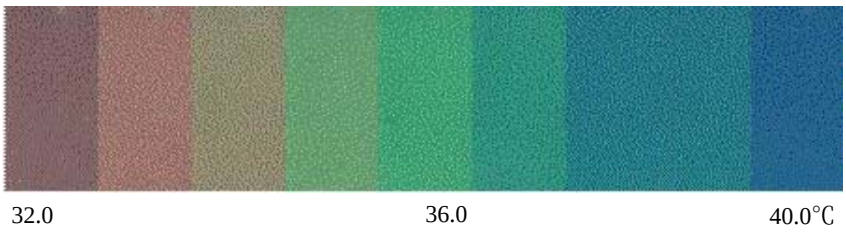

Calibration of temperature

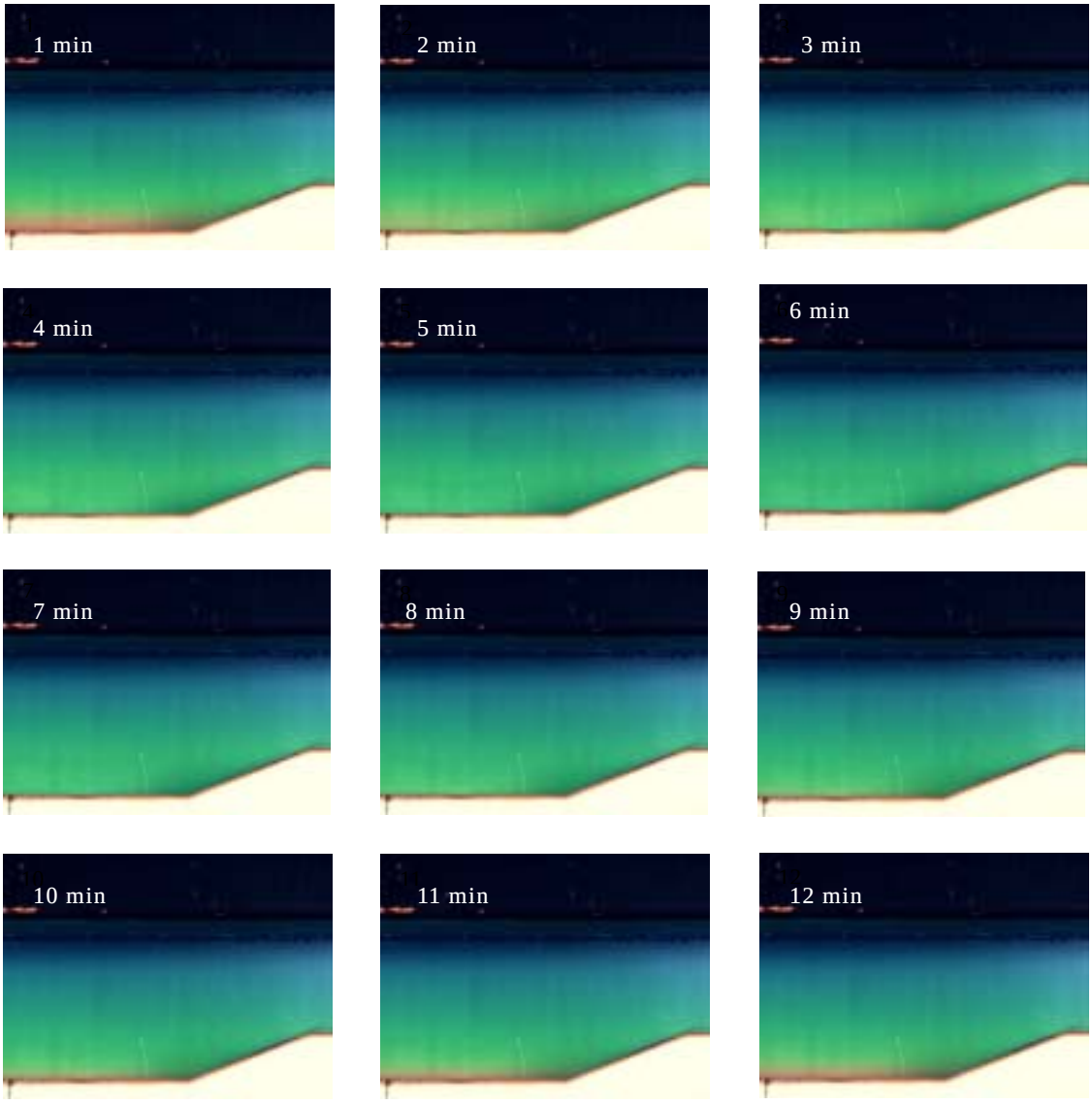

Fig. 9 The temperature measurement of the water tank experiment by using crystalline sheet

The temperature obtained by numerical model in water tank experiment is shown in Fig.10. The simulated temperature results show the temperature distribution of water tank experiment.

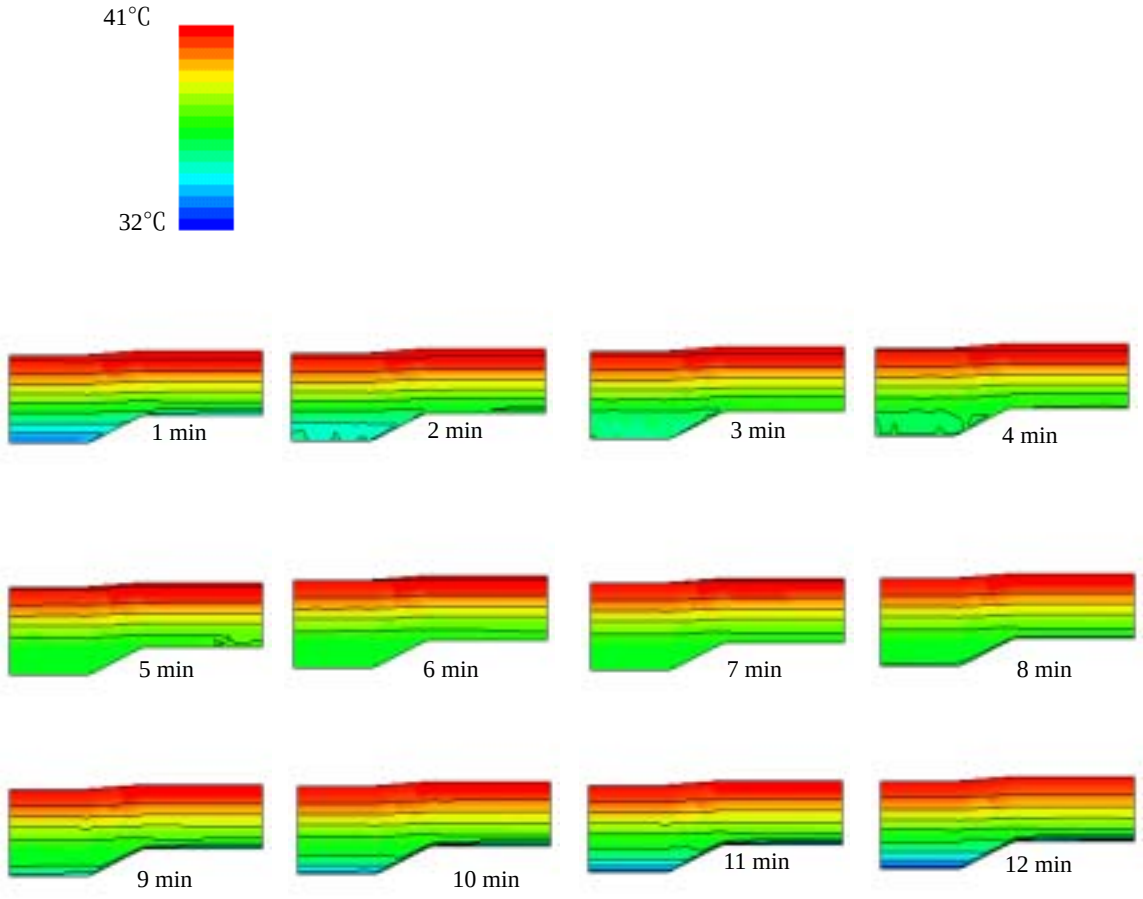

Fig.10 The temperature distribution of water tank experiment by numerical calculation

When Fig. 9 and Fig. 10 are compared, the temperature distribution of water tank experiment obtained by thermo crystal liquid sheet and numerical calculation matches.

The comparison of temperature measurement in water tank experiment by thermo couples and numerical calculations are also compared which is shown in Fig. 11. During early morning and night time, there is slight difference(Max. 1℃) in temperature measured in water tank experiment by thermocouples and numerical calculation, but at day time, temperature matches in both cases.

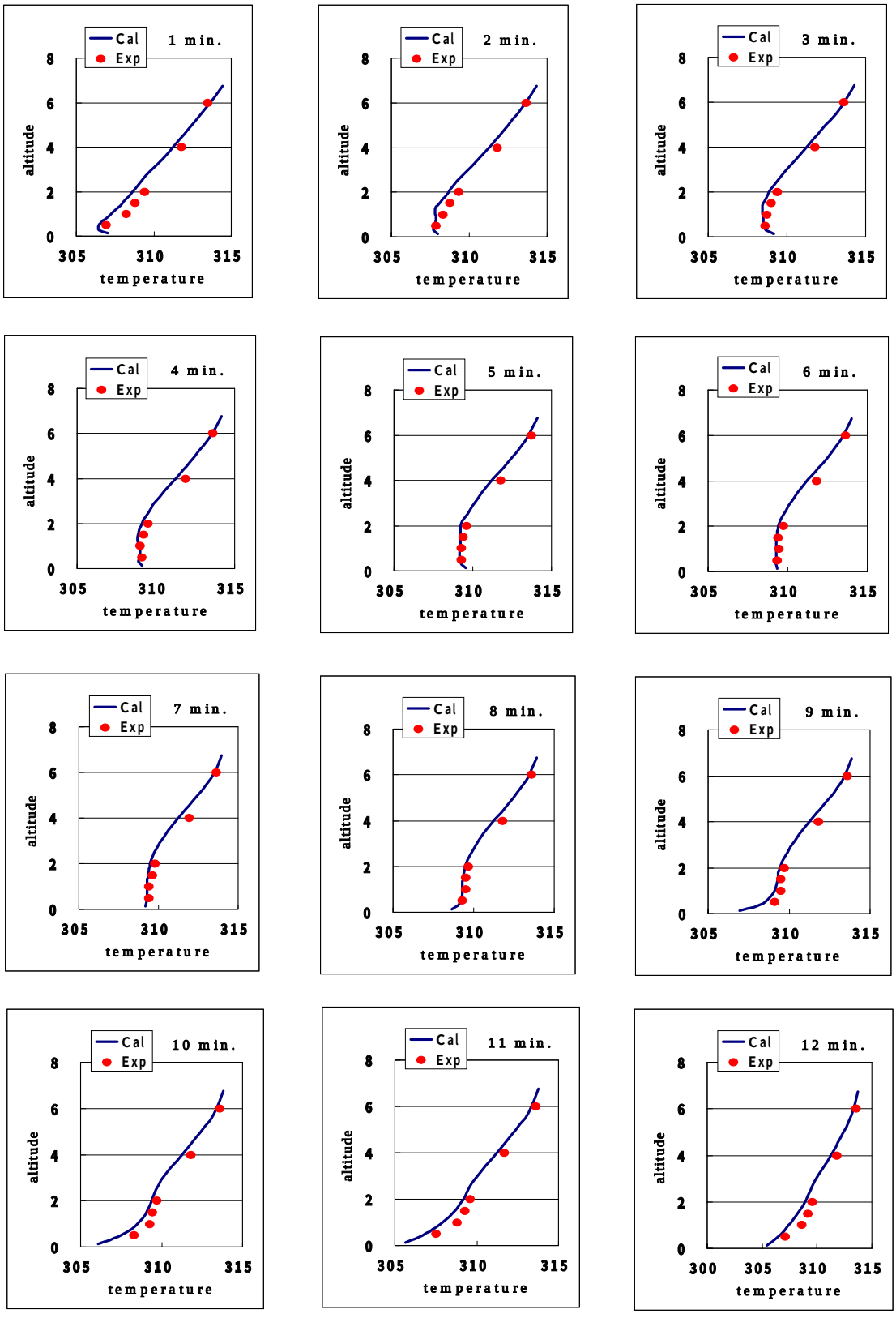

Fig.11 Comparison of temperature measurement in water tank experiment by thermo couples and numerical model each minute of experiments.

4.2 Flow field

The result of the flow field in water tank experiment is shown in Fig.12. The flow field obtained by the numerical calculation was shown in Fig. 13. The time displayed in Fig.12 and 13 correspond to the period of Fig.5. The updraft wind on the slope (valley wind) and Bernard convection occurred when the bottom temperature was increased as shown in the images of 2,3,4 and 5 minute of Fig.12 and 13. The downdraft wind on the slope (valley wind) occurred when the bottom temperature was decreased as shown in images of 9,10,11 and 12 minute of Fig. 12 and 13. The counter flow occurred above the valley and later, the downdraft wind became low at the bottom of the valley. The flow field agrees in the experiment (Fig.12) and numerical calculation (Fig.13) due to the quite similar image results in both cases.

During the daytime from 2 minute to 5 minute in water tank experiment, the pollution concentration in valley is considered low due to the presence of updraft wind and Bernard convection but at nighttime, the pollution concentration is considered high due to the formation of the inversion layer and downdraft wind in valley. The NO_2 and TSP concentration data in Fig. 1 and Fig.2 agrees with this mechanism.

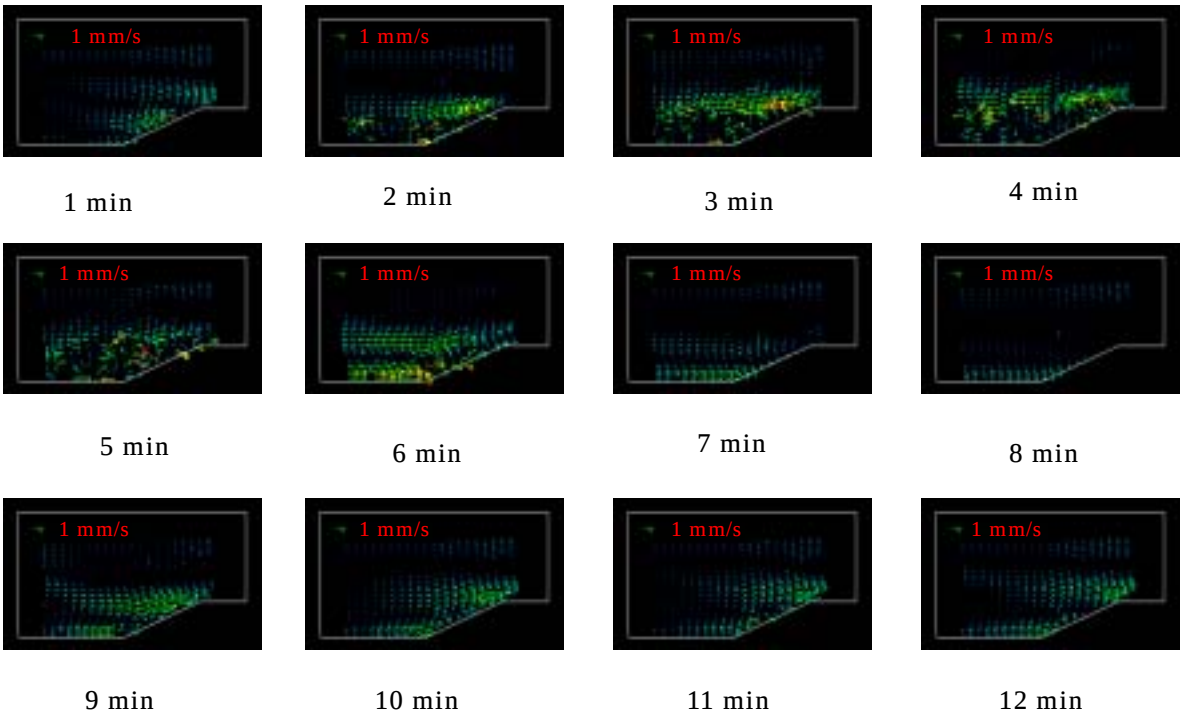

Fig.12 Flow field extracted from visualized images after each 1 min. of interval in water tank experiment

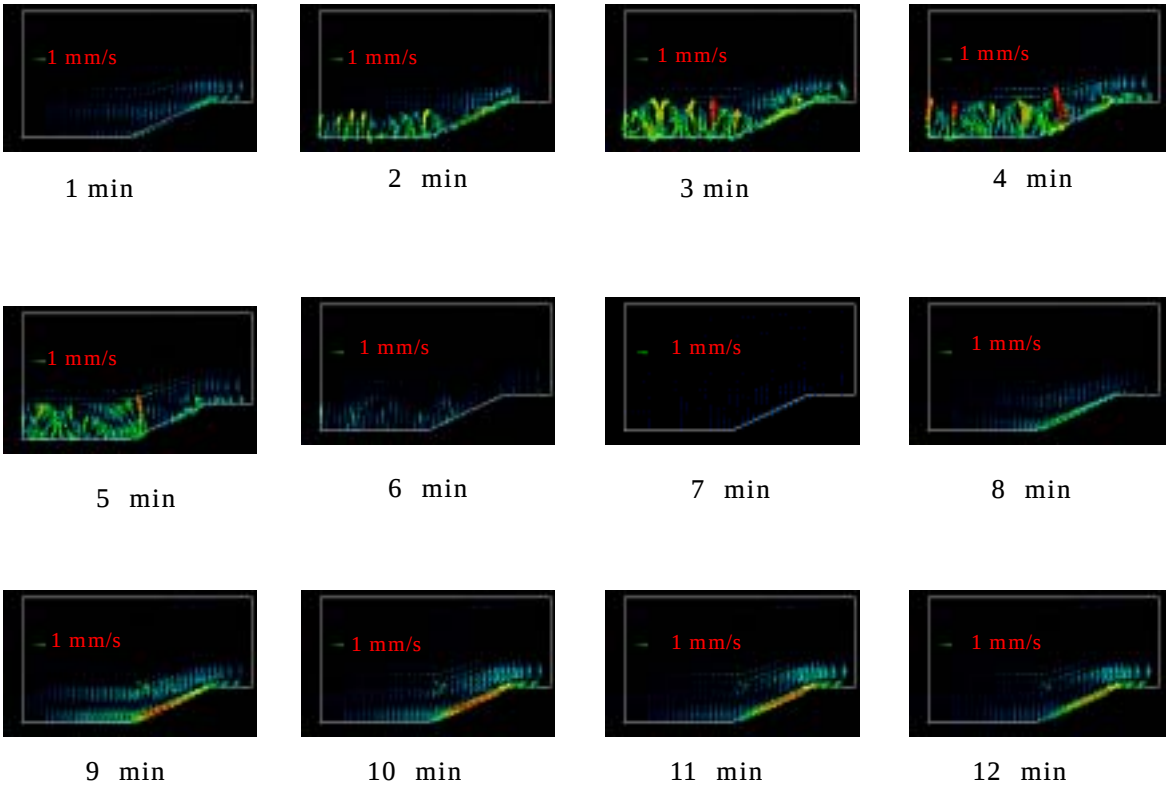

Fig. 13 Flow field of water tank experiment obtained from numerical calculation

5. Conclusion

The winter high air pollution mechanism of the Kathmandu valley was realized by water tank experiment. The flow field of Kathmandu valley was studied by PIV. Updraft wind and Bernard convection occurred during the daytime. Downdraft wind and inversion layer occurred at nighttime. The velocity field and temperature measured in water tank experiment agree with the result of numerical calculation.

References

[1] Shrestha, M. L., Kondo, A., and et.al., Diurnal Variation of Air Pollution Concentration during Winter in Katmandu Valley, Air Pollution 2002, 2002

[2] S. Mitsumoto, Ueda, H. and Ozoe, H., A Laboratory Experiment on the Dynamics of the Land and Sea Breeze, , 40, 1228-1240 ,1983

[3] Kondo, A., Kaga, A. and et.al., Analysis of Sea and Land Breeze in a Water Tank Experiment and Numerical Simulation and Influence of its Flow Fields on Mass Diffusion, J.Jpn. Soc. Atmos. Environ., 35, 355-367, 2000 (in Japanese)

[4] Kaga, A., Inoue, Y. and Yamaguchi, K., Pattern Tracking Algorithms Using Successive Abandonment, J. of Flow Visualization and Image Processing, 1, 283-296 1993

[5]Ueda, H.: Effects of External Parameters on the Flow Field in the Coastal Region -- A Linear Model -J. Climate and Appl. Meteor., 22, 312-321 1982,